The EMBO Journal vol.15 no.10 pp.2343–2355, 1996

A novel immunogold cryoelectron microscopic approach to investigate the structure of the intracellular and extracellular forms of vaccinia virus

Norbert Roos[1], Marek Cyrklaff[2], Sally Cudmore, Rafael Blasco[3], Jacomine Krijnse-Locker and Gareth Griffiths[4]

Cell Biology Programme and [2]Biological Structures Programme, European Molecular Biology Laboratory, D-69012 Heidelberg, Germany, [3]Centro de Investigacion en Sanidad Animal, INIA-MAPA, Valdeolmos, E-28130 Madrid, Spain and [1]Electron Microscopy Laboratory for Biology, University of Oslo, Blindern 0316 Oslo 3, Norway

[4]Corresponding author

We introduce a novel approach for combining immunogold labelling with cryoelectron microscopy of thin vitrified specimens. The method takes advantage of the observation that particles in suspension are concentrated at the air–water interface and remain there during the subsequent immunogold labelling procedure. Subsequently, a thin aqueous film can be formed that is vitrified and observed by cryoelectron microscopy. In our view, a key early step in the assembly of vaccinia virus, the formation of the spherical immature virus, involves the formation of a specialized cisternal domain of the intermediate compartment between the endoplasmic reticulum and the Golgi. Using this novel cryoelectron microscopy approach, we show that in the intracellular mature virus (IMV) the core remains surrounded by a membrane cisterna that comes off the viral core upon treatment with dithiothreitol, exposing an antigen on the surface of the viral core. Complementary protease studies suggest that the IMV may be sealed not by membrane fusion but by a proteinaceous structure that interrupts the outer membrane. We also describe the structure and membrane topology of the second infectious form of vaccinia, the extracellular enveloped virus, and confirm that this form possesses an extra membrane overlying the IMV.

Keywords: cryoelectron microscope/immunogold labelling/vaccinia virus

Introduction

The classical view of the assembly of poxviruses such as vaccinia was that it involved a *de novo* synthesis of a single viral membrane in the cytoplasm (Dales and Mosbach, 1968). This assumes that the membrane arranges itself to build the first, morphologically distinct form of the assembling virus, the spherical immature virus (IV). The IV then encloses the viral DNA and develops further into the first infectious form, the brick-shaped, intracellular mature virus (IMV), previously referred to as the intracellular naked virus (reviewed by Dales and Pogo, 1981).

Recently, we have challenged this classical view and argued that both the IV and IMV possess two distinct, but tightly apposed membranes, a consequence of their being derived from a specialized domain of the endoplasmic reticulum (ER), the intermediate compartment (Sodeik *et al.*, 1993; Krijnse-Locker *et al.*, 1994). Although the presence of two tightly apposed membranes in the IV is difficult to show without using protease treatment, two distinct membrane profiles are visible in electron microscopy (EM) sections of the IMV using both thawed cryosections of fixed cells and epoxy resin sections (Dales and Pogo, 1981; Sodeik *et al.*, 1993). This poses a dilemma (see below).

Whereas the IMV is not found in appreciable amounts in the extracellular medium of infected cells (except, presumably upon cell death), the extracellular enveloped virus (EEV) is actively released from the cell (Appleyard *et al.*, 1971; Payne, 1978; Payne and Norrby, 1978). In the process of EEV assembly, the IMV acquires two additional membranes derived from the *trans* Golgi network (TGN) cisternae forming an intracellular enveloped virus (IEV) that possesses four distinct membrane profiles in thin sections (Hiller and Weber, 1985; Schmelz *et al.*, 1994). This second, cisternal envelopment of the IMV is critically dependent on at least two membrane or membrane-associated proteins: (i) a 14 kDa protein on the surface of the IMV (Rodriguez and Esteban, 1987; Rodriguez and Smith, 1990; Sodeik *et al.*, 1995) and (ii) a 37 kDa palmitylated protein in the cisterna derived from the TGN, which behaves as an integral membrane protein (Hiller and Weber, 1985; Schmutz *et al.*, 1991, 1995) (Table I). Two other integral membrane proteins of the wrapping cisterna, p21 and p42-50, are seemingly also essential for the formation of the four-membraned IEV (Duncan and Smith, 1992).

According to the available data, the IEV fuses with the plasma membrane, releasing the three-membraned EEV into the extracellular medium (Payne and Kristenson 1979; Hiller *et al.*, 1981; Schmelz *et al.*, 1994). The movement of the IEV through the cell in order to reach the plasma membrane is caused by the formation of filamentous actin tails behind the virus particles. These actin tails closely resemble the structures first described for *Shigella* bacteria (Clerc and Sansonetti, 1987). On reaching the plasma membrane, the virus particles project outward from the cell at the tip of virally induced actin microvilli (Cudmore *et al.*, 1995). Following exocytic fusion, the released EEV particles expose the lumenal domains of the EEV-specific membrane-spanning glycoproteins. It is not yet clear whether any part of the 37 kDa protein is also exposed on the EEV surface, but it is predicted (and recently shown; Schmutz *et al.*, 1995) that the major part of this

protein would be cytoplasmically disposed, both on the plasma membrane (after IEV fusion) and in the space between the EEV outer and inner membranes. Since both infectious forms of vaccinia, the IMV and the EEV (that has one additional membrane relative to the IMV), are thought to enter the cell by fusing with the plasma membrane of the host cell (Doms *et al.*, 1990), one has to assume that two different mechanisms of viral disassembly are employed. When the IMV infects cells it appears to release the viral core into the cytoplasm (Dales, 1963) where the early transcription machinery present in the viral core is activated. This event can be reconstituted *in vitro* (Kates and McAuslan, 1967). However, if the EEV fuses with the plasma membrane during infection it will seemingly put an intact IMV particle into the cytoplasm. The question therefore arises, how can an IMV particle previously assembled in the cytoplasm of an infected cell be disassembled in the cytoplasm of the cell it infects?

The novel technique developed during this study was to combine cryo EM with a colloidal gold-based immunolabelling procedure which was then used to investigate the structure of purified fractions of both the IMV and EEV. For the IMV, a preliminary cryo EM study has already been described (Dubochet *et al.*, 1994). Two significant findings were reported; (i) the images of the IMV confirmed earlier data based on chemically fixed material and showed two membrane-like domains that were separated by a layer of spike-like structures, and (ii) upon treatment of the IMV with NP-40 and dithiothreitol (DTT), a treatment used extensively to prepare biochemical amounts of viral cores (Easterbrook, 1966; Holowczak and Joklik, 1967), the ensuing particles were covered by an array of spike-like projections morphologically similar to structures first described in conventional Epon sections in both the IV and IMV by Dales and Siminovitch (1961) and Dales (1963). Beneath this palisade of 'spikes', an electron-dense layer is seen.

Two different models can be envisaged to account for the observed features (Figure 1). First, the two bilayers of the IMV seen in both conventional Epon sections and by cryo EM are the result of a separation of the two tightly apposed IV membranes (Figure 1, model B). In this case, the inner of these two membranes will constitute the core 'membrane'. Alternatively, the outer 'membrane' of the IMV is, as in the IV, composed of two tightly apposed membranes (Figure 1, model A). In that case the distinct core 'membrane' must also be accounted for. One of our major goals at the outset of this study was to distinguish between these two models.

Cryo EM of thin films of vitrified suspensions is by far the most suitable method for observing delicate biological particles for high resolution EM (Dubochet *et al.*, 1988). In most cases, it helps to overcome the usual preparation artefacts due to chemical fixation, staining and dehydration. In this method, a drop of suspension is applied directly to a grid or a grid coated with a perforated carbon film. It was found recently that particles suspended in the solution tend to adsorb to, and concentrate at, the air–liquid interface in the holes of the grid (Johnson and Gregory, 1993). Most of the drop of suspension can be replaced by other buffers without loss of the particles adsorbed at the surface (Cyrklaff *et al.*, 1994). These adsorption properties allow one to perform chemical treatments, staining and/or immunolabelling of the adsorbed particles under extremely mild conditions. Finally, most of the drop is removed with blotting paper, and the residual thin layer containing the treated particles can be vitrified and observed in the cryoelectron microscope.

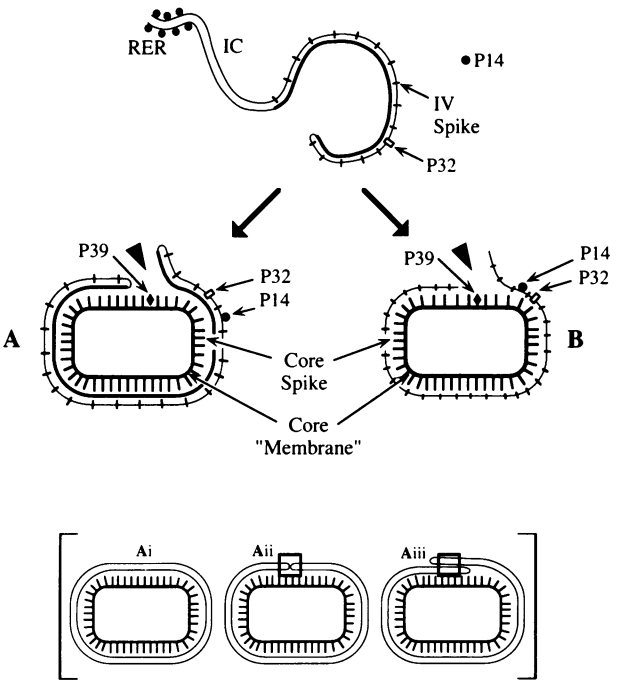

Fig. 1. Models of IMV formation and location of key proteins in relation to the enwrapping membranes of the intermediate compartment (IC) that we propose to be directly continuous with the rough endoplasmic reticulum (RER). The upper part of this model is based on our previous study (Sodeik *et al.*, 1993; for a review, see Griffiths and Rottier, 1992) and argues that the IV is a highly apposed cisterna derived from the IC. In model (A), the key point is that the IV cisterna remains tightly apposed to and overlies the spikes which are on the surface of the core. A second set of (8 nm) surface spikes is evident on the surface of the IMV. In model (B), the spikes are shown as lumenal structures. In both models, DTT is envisaged as exerting its effect by reducing intra-lumenal S–S bonds and thereby affecting intra-lumenal protein–protein interactions. In model (A), the composition of the core 'membrane' is left open, while in (B) it represents the inner membrane of the IV-derived cisterna after a process of separation. The results in this study argue strongly against model (B); nevertheless, the precise structure of the outer surface remains to be solved. Based on both the structural data and the accessibility of core proteins to proteases, we suggest that the cisterna is not fused with itself (Ai) but may be glued together by a proteinaceous plug. The absence of any structural data for a 'pore' (Aii) makes us favour the view that the putative proteinaceous structure may be covered by an overlap in the cisterna (Aiii).

Table I. Location of membrane proteins in IMV and EEV

Virus	Protein	Gene	Location
IMV	p14	A27L	Outer surface of IMV cisterna
	p32	D8L	Outer surface of IMV cisterna
	p39	A4L	Surface of the core
EEV	p37	F13L	Inner surface of the outer membrane of EEV
	p42	B5R	Surface of the EEV

Here we have taken advantage of this observation in order to combine chemical treatment, uranyl acetate staining and immunogold labelling, employing a spectrum of antibodies, with cryo EM using different forms of vaccinia virus. Using this approach, we show that treatment of purified IMV with the reducing agent DTT disrupts the IMV in a reproducible fashion; it appears to loosen the interactions between the two outer membranes and thereby facilitates a peeling off of the cisterna. In this process, a 39 kDa core surface protein (Table I), that is inaccessible to its antibody in intact IMV, becomes exposed. By use of structural disruption of the EEV, we could also confirm that this viral form contains one additional membrane (relative to the IMV) in which the membrane-spanning protein, p42 (Table I), is exposed on the outside. A second integral membrane protein, p37 (Table I), is buried cytoplasmically in the space between the surface of the IMV and the EEV membrane. Collectively, our data suggest that, if the EEV fuses with a cell and releases an intact IMV into the cytoplasm, the presence of a reducing environment may be sufficient to induce an uncoating of the IMV into the transcription-competent core stage.

Results

Our rationale in this study was to gain insights into the way vaccinia IMV and EEV are assembled. In order to achieve this, we used a controlled process of disassembly of the viral particles and an electron microscopical preparation procedure in which the resulting viral structures are best preserved. Clearly, the best method which satisfied these requirements was the 'fully-hydrated' method for cryo EM (Dubochet *et al.*, 1988). However, unlike most (periodic) viruses that have been studied by cryo EM (e.g. Stewart *et al.*, 1991), both forms of vaccinia are relatively large. The roughly brick-shaped particles have approximate dimensions of 350×250×150 nm and are, thus, perhaps, at the limit for this method. Since both infectious forms show at least two membrane profiles, it was clear that for interpreting the images the use of antibodies against proteins known to be localized to specific parts of the virus would be needed.

Whereas for small viral particles, any bound IgG molecules, or even individual Fab fragments, can be resolved without additional markers, for a large particle such as vaccinia an electron-dense marker was essential. For this purpose, 5 and 10 nm gold particles conjugated to protein A were used for most experiments. We first visualized either (unlabelled) intact IMV or viral cores (operationally defined), prepared using NP-40 plus DTT, by cryo EM. Treatment of IMV particles with NP-40 and a reducing agent such as DTT is a classical procedure for preparing vaccinia core particles (Joklik, 1964; Easterbrook, 1966) that are transcription active *in vitro* (Kates and McAuslan, 1967). For both types of particles (IMV and cores), the images obtained (Figure 2A–C) are similar to those observed by Dubochet *et al.* (1994), with the IMV displaying two electron-dense layers that are presumably membranes. The space between these layers contains the ~20 nm spike-like projections. When the cores were visualized, these spikes were visible as projections on their surface (Figure 2B and C). In addition, we observed an additional set of spike-like protrusions of an average length of ~8 nm on the surface of the IMV (Figure 5A). The molecular identity of these structures is unclear at present.

For immunogold labelling, we first used two antibodies that recognize proteins on the surface of the IMV, namely the peripheral membrane protein p14 and the integral membrane protein p32 (Table I). For labelling the surface of the viral core, we used an antibody against p39 (Table I), a protein first described by Rodriguez *et al.* (1987) and which we have characterized in more detail (S.Cudmore *et al.*, in preparation). In the latter study, labelling of viral particles followed by negative staining shows clearly that α-p39 does not label the intact IMV but strongly labels the surface of the (NP-40 plus DTT-treated) viral cores. Antibodies against this protein also label the surface of the isolated natural cores that appear in the cytoplasm during the viral infection process (E.Snijder *et al.*, in preparation). These observations are confirmed in the present study (see below).

Treatment of IMV with DTT

The two membranes in the immature virus IV are so tightly apposed that they appear as a single membrane in most thin section images (see Dales and Pogo, 1981; Sodeik *et al.*, 1993). However, in the IMV, two distinct layers are evident in both thawed cryosections of aldehyde-fixed cells and by cryo EM of intact IMV virus (Figure 2A; Sodeik *et al.*, 1993; Dubochet *et al.*, 1994; see also Dales and Pogo, 1981). Prominent spike-like structures are especially visible in the space between these two layers in vitrified IMV preparations (Dubochet *et al.*, 1994; Figure 2B). The question therefore arises as to whether the two tightly apposed membranes seen in the IV separate in the IMV. In this case, the spike-like projections would be lumenal structures that perhaps cross-link the two membranes of the cisterna (Figure 1, model B). Alternatively, the IMV has an outer layer that, as in the IV, is actually composed of two tightly apposed membranes and it possesses an additional electron-dense layer close to the viral DNA. If this is the case, the spikes must be cytoplasmically disposed structures, that might cross-link the inner, cytoplasmic surface of the cisterna with the surface of the core outer layer (Figure 1, model A).

To try to resolve this issue, we looked for treatments that would disrupt the organization of the different layers, without destroying membrane structure. Inspired by the work of Easterbrook (1966), we found that the most striking effect was obtained using DTT, a treatment we expected to disrupt any disulphide bonds in the virus. The same effects were also seen with 2-β-mercaptoethanol (2-β-ME; results not shown). As shown in Figure 3, incubation of IMV on the EM grid with 20 mM DTT for short periods (5–30 min) resulted in a statistically significant swelling of the IMV [untreated average (n = 25): length 338 nm ± 13 nm (SD), width 267 nm ± 18 nm (SD); treated average of the non-disrupted particles (n = 25): length 356 nm ± 15 nm (SD), width 289 nm ± 15 nm (SD)]. Under these conditions the IMV surface antigens p14 (not shown) and p32 (Figure 4) remained fully exposed, with essentially no labelling seen with the antibodies against either p39 or with a control, irrelevant antibody. However, with increasing times of treatment, a higher percentage of particles became disrupted and the

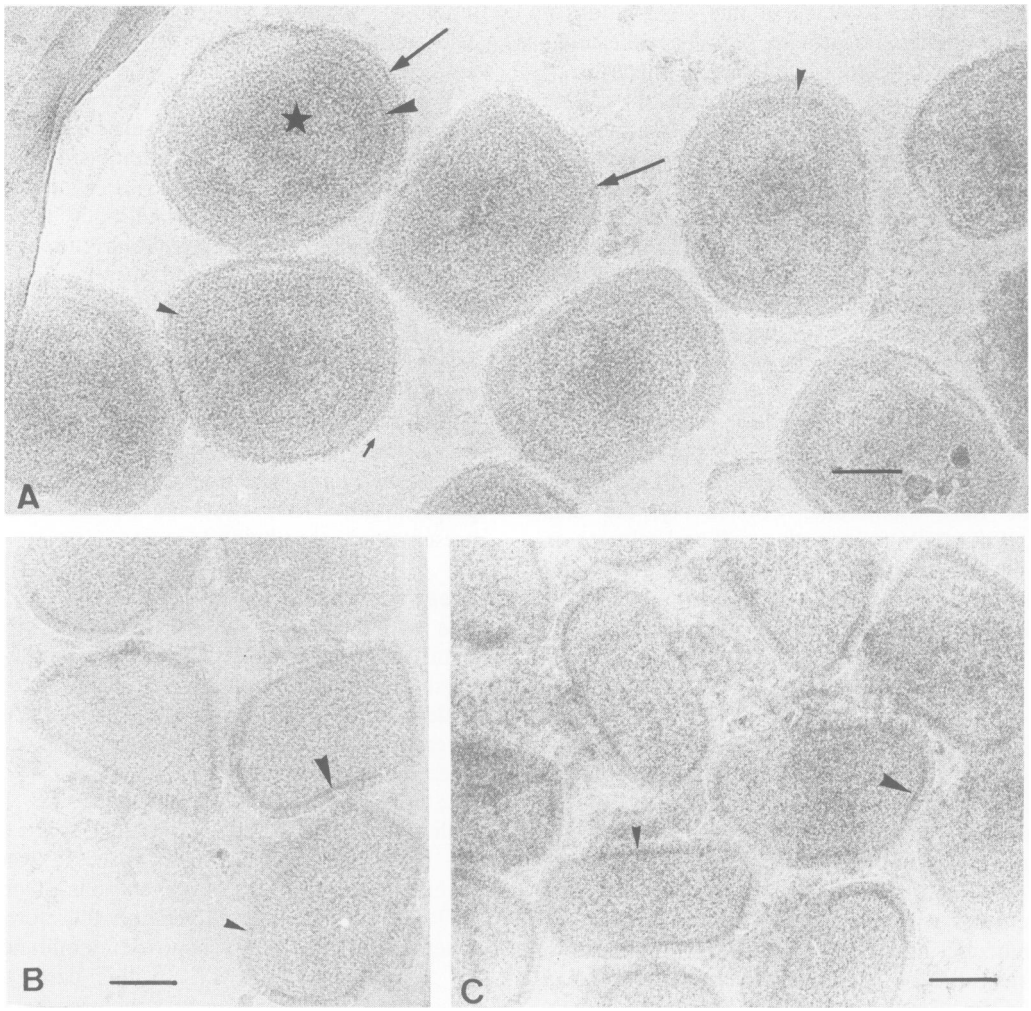

Fig. 2. Vitrified IMV particles: (**A**) untreated IMV particles, (**B**) and (**C**) isolated cores after NP-40/DTT treatment. The large arrows show the outer membrane of the IMV, while the large arrowhead indicates the core outer layer. The small arrow points to the IMV surface spike projections, while the more prominent 20 nm spike on the surface of the core is indicated by small arrowheads. The asterisk depicts one of the very few partially disrupted IMVs found. We believe that the extraneous material surrounding the cores in (B) and (C) represents remnants of the outer cisterna which are not extracted by the detergent (bar = 100 nm).

particles labelled for p39 (see below). Representative images of this disruption process are shown in Figure 3.

The disruption of the IMV with DTT was also visualized by a number of novel modifications of the bare-grid method. First, the virus could be chemically cross-linked using brief exposures (seconds to minutes) to low concentrations of aldehydes (not shown). This approach became more important for the studies with the EEV (see below). Second, the viruses, either with or without DTT treatment, could be exposed for a few seconds to low concentrations of uranyl acetate, which subsequently was replaced by pure water prior to freezing (positive staining; Figures 3F–I and 4). This treatment showed that, whereas intact IMV were refractory to the stain, the stain clearly entered the particles that had been affected by DTT. Figure 3 shows different images of the DTT-induced disruption, a process which ultimately exposes the viral core, and thus may resemble the natural uncoating process that occurs during infection. In addition to the swelling with DTT, we also noted a separation of the outer membrane(s). This separation process often appeared to be initiated at the corner of the particle (Figure 3A and F). In Figure 3G, the two membrane profiles of the outer cisterna are evident (see also Figure 3E), while Figure 3F, G and I suggests that DTT induces a peeling off of this outer cisterna. In some cases, this outer cisterna forms long, 20 nm diameter tubules resembling the so-called 'surface tubular elements' first described by Stern and Dales (1976). In all cases where disruption occurred, the surface of the core became exposed, as evidenced by the core spike elements (Figure 3A, C–F, H and I). Occasionally, the cores themselves also appear to become disrupted by DTT (Figure 3I).

In order to examine this DTT-induced uncoating process in more detail, we next analysed the pattern of labelling for the IMV surface antigens p14 and p32 and the core surface protein p39 (see Table I) on such disrupted particles. A summary of the key findings is as follows: p39 was localized exclusively to the exposed core, identified by the presence of the 20 nm spike-like projections on their surface (Figure 5E–F). In contrast, antibodies against the surface membrane proteins p14 and p32 labelled only the outer membrane of the IMV (Figure 5A–D). Following disruption of the outer cisterna, the labelling for p14 and p32 was restricted to the membrane fragments that were

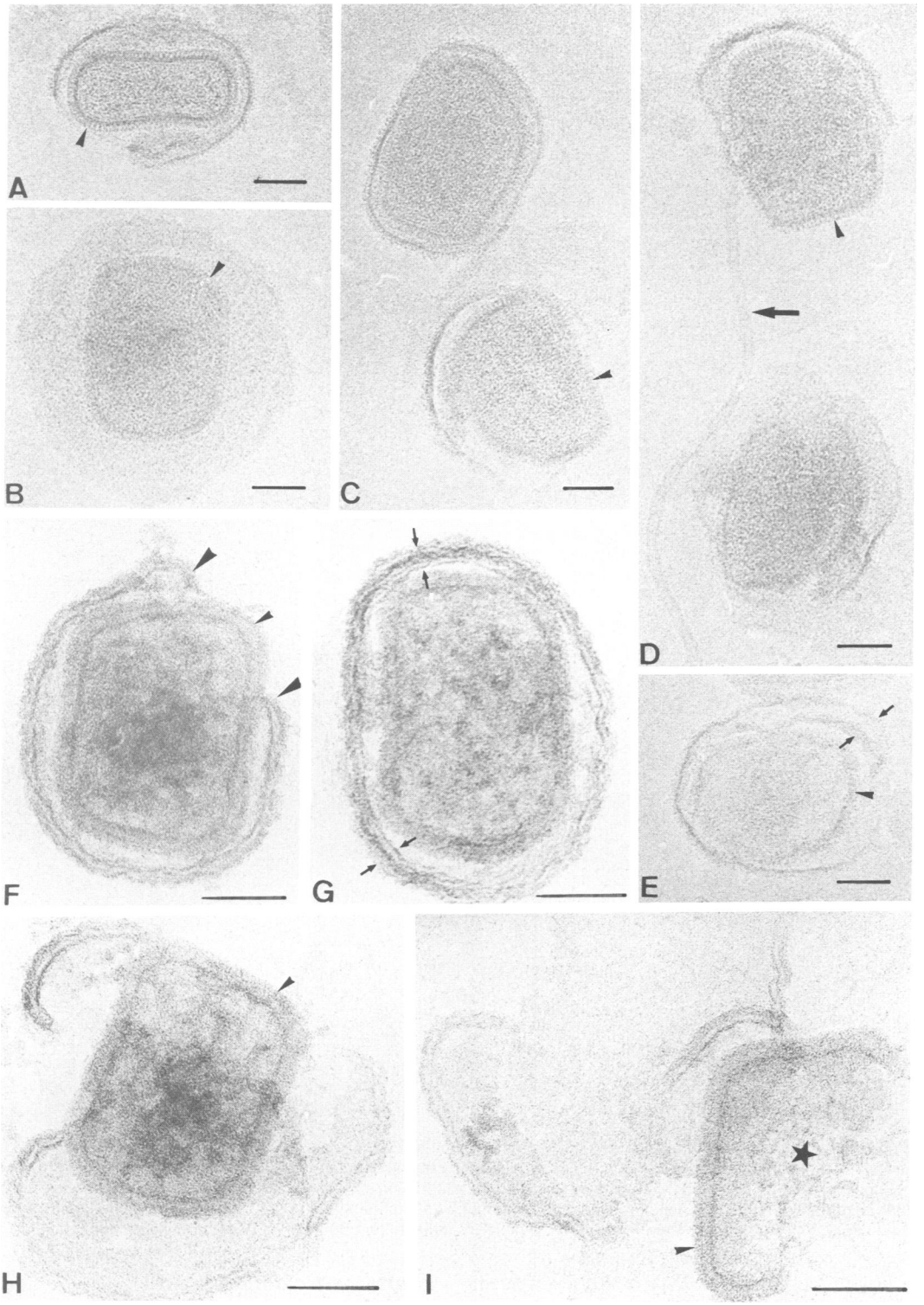

Fig. 3. Effect of 20 mM DTT at 37°C for 10 min (**B**, **C**, **F** and **G**) or 30 min (**A**, **D**, **E**, **H** and **I**) on intact IMV. (A–E) show unstained cryo EM preparations, while (F–I) are preparations stained for a few seconds with 0.3% uranyl acetate. The initial effects of DTT include swelling of the outer cisterna (B, D and G). Subsequently, the particle appears to uncoat (A, C–F, H and I), exposing the major core spike (small arrowheads). In (G) and (E) the small arrows reveal the two membranes of the outer cisterna. In (F) the large arrowheads indicate the ends of the cisternae that appear to be peeling off the core surface. The tubule seen in (D) (arrow) is probably an artefact of the DTT-induced uncoating process that resembles the surface tubular elements seen in classical negative stain images (bar = 100 nm).

attached to the cores devoid of labelling. The labelling density seen on such membrane fragments was similar to that seen on the surface of intact IMV.

In the next series of experiments, we asked whether the approach introduced here for single immunolabelling could also be applied for a double labelling procedure. For this, the IMV was first labelled with antibodies against one of the surface membrane proteins p14 or p32 (Table I),

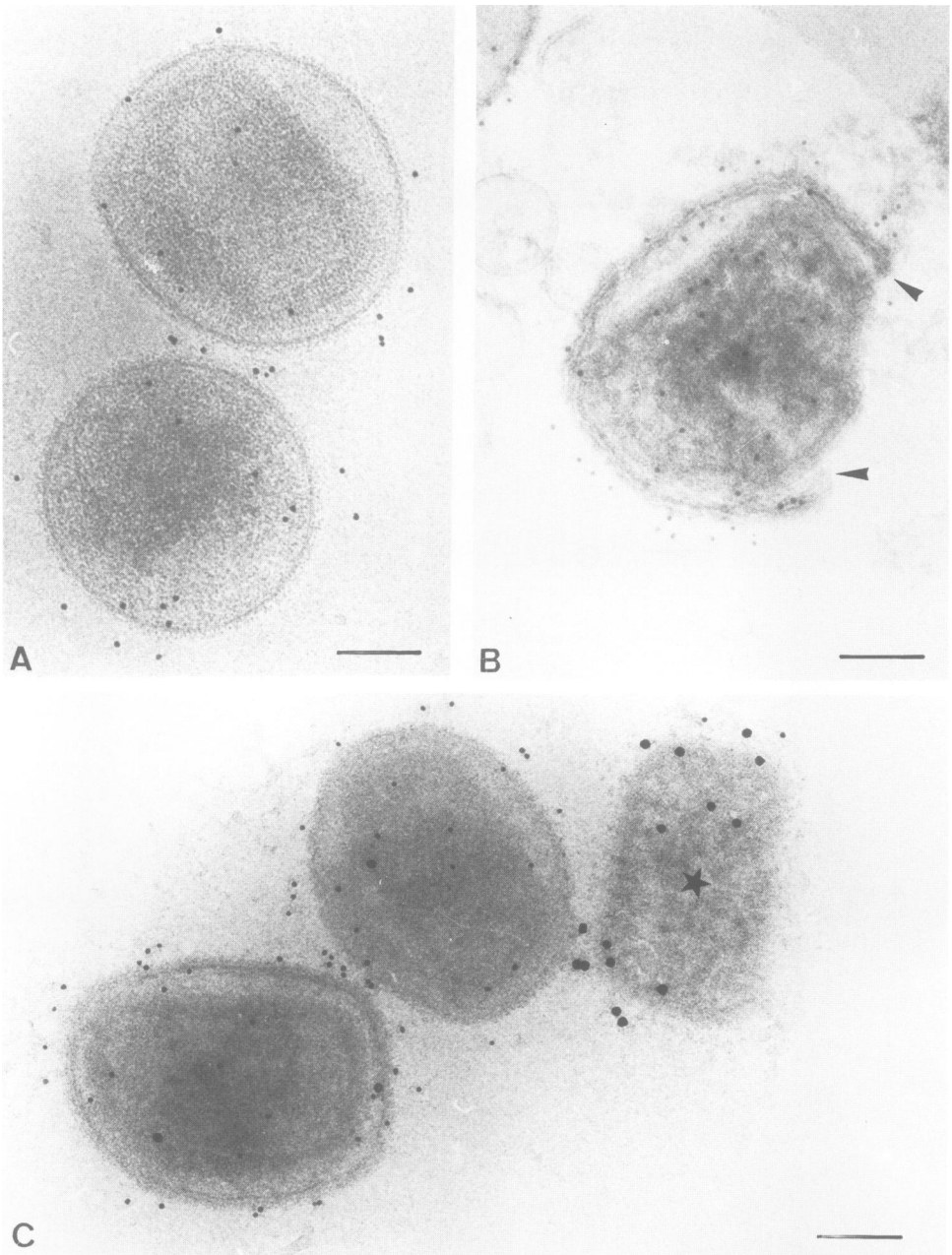

Fig. 4. (**A**) and (**B**) IMV particles treated with DTT (20 mM for 10 min) and labelled for p32. In (A) the particles are swollen while in (B) disruption is evident. The preparation in (B) and (C) is stained with 0.3% uranyl acetate. The arrowheads indicate the ends of the outer cisterna. (**C**) Double labelling experiment. The intact IMV was first labelled with p32 followed by 5 nm protein A–gold. The particles were treated subsequently with 20 mM DTT for 10 min and labelled for p39 followed by 10 nm protein A–gold. The image selected shows two intact particles (left) adjacent to a released core (asterisk). Whereas the intact IMV labels strongly for p32 the core labels strongly for p39.

followed by protein A–gold. The IMV was then treated with DTT, briefly fixed (<1 min) with glutaraldehyde (Slot *et al.*, 1991) and then labelled with an antibody against another vaccinia protein, or with control antibodies, followed by a different size protein A–gold complex. As shown in Figure 4, this double labelling procedure facilitated a visualization of the disruption of the IMV by DTT. Whereas the outer membranes labelled for p14 and p32, the core, which became exposed following disruption, could be labelled specifically only with α-p39 (Figure 4C). The finding that DTT treatment leads to the exposure of epitopes on a core surface protein argues strongly for model A rather than B in Figure 1.

Protease treatment of IMV

The above experiments with DTT suggested that the outer membrane of the IMV might not form a completely uniform cover around the IMV, i.e. that the outer cisterna that enwraps the viral core may not have fused with itself (Figure 1, model Ai). We therefore asked whether this cisterna could be sealed by a proteinaceous structure such as a 'pore' or 'focal contact' (Figure 1, model Aii or Aiii). If so, such a structure might be accessible to protease treatment. In extensive (unpublished) studies with proteases, we had noticed that different IMV preparations behaved very irreproducibly towards proteases. In many experiments, relatively high concentrations of proteases

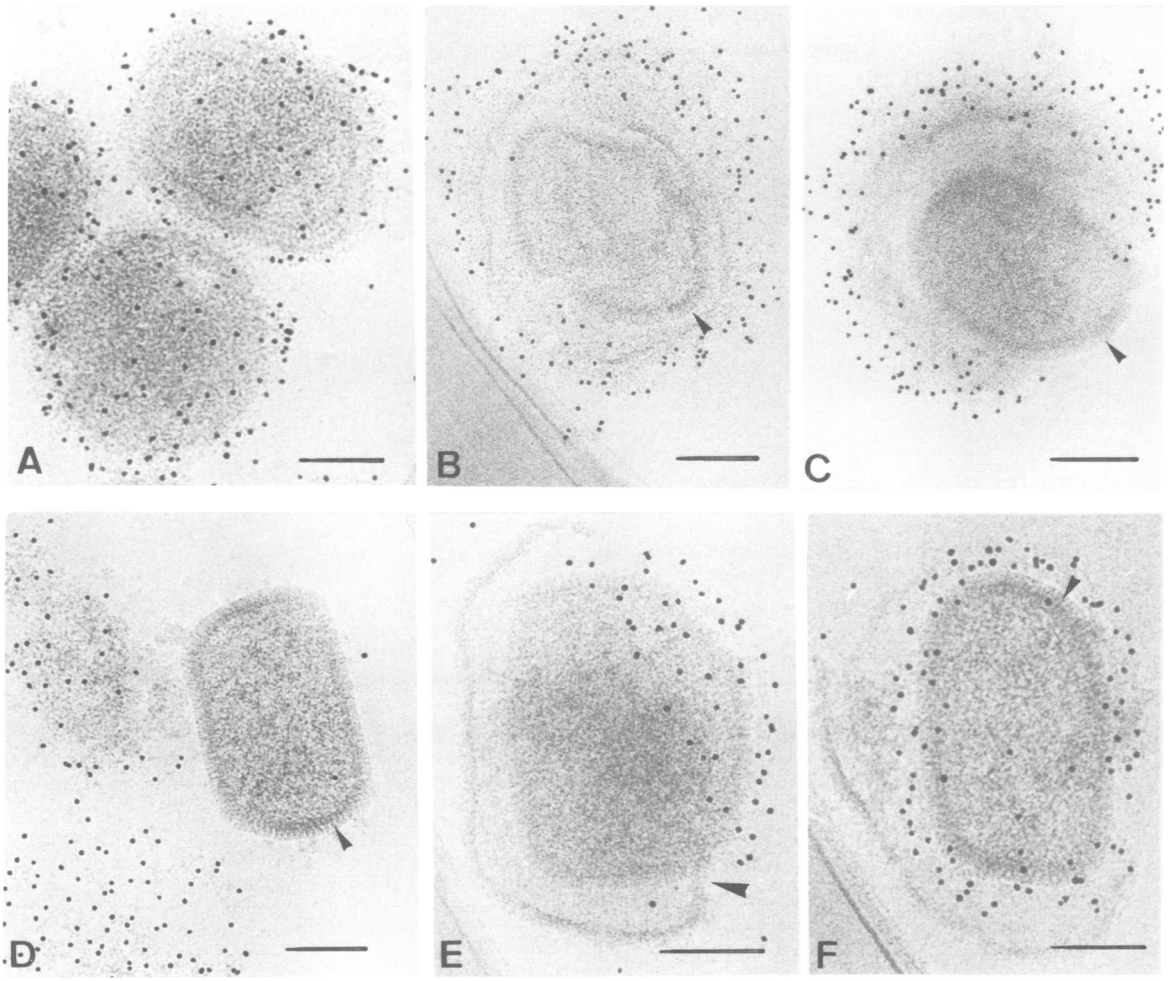

Fig. 5. (**A**) Undisrupted IMV particles labelled with α-p14. (**B–D**) IMV particles exposed to DTT (20 mM for 30 min at 37°C) prior to immunolabelling with α-p14; (**E**) and (**F**) labelling for p39. These data show that α-p14 labels the outer membrane of IMV but not the exposed core, whereas α-p39 labels the core but not the outer membrane (bar = 100 nm).

digested IMV surface protein (such as p14) without affecting core proteins such as p4a or p39; in others, however, core proteins became digested within ~2 h of treatment.

We therefore carried out a systematic study using two proteases, proteinase K (4°C) and trypsin (37°C), and assayed their effects both by biochemical analysis and by negative staining EM (Figure 6). We emphasize that the goal of the latter approach in this study was simply to evaluate whether or not stain entered the particle, not to provide any structural details. Whereas the majority of intact IMV particles exclude stains such as uranyl acetate, this stain can enter particles that have been disrupted, for example with DTT, as mentioned.

IMV were treated with 100 or 200 μg/ml of either proteinase K at 4°C or trypsin at 37°C for either 1 or 2 h. In this experiment, treatment with 200 μg/ml proteinase K (4°C) for 2 h, a concentration which completely digested the surface protein p14 after 30 min, failed to digest the core proteins significantly (not shown). Similarly, by negative staining, there was little difference in the staining appearance between untreated particles and those treated with 200 μg/ml proteinase K for 2 h (Table II). In the case of trypsin at 37°C, all treatments completely removed the surface protein p14 (Figure 7). In contrast, at least 2 h was needed to show visible signs of degradation of the core proteins p39 and p4a. By 4 h, these proteins were essentially completely digested (Figure 7). These results were again complemented by the EM negative staining approach (Table II). The images from this experiment also showed a significant fraction of particles that were obviously disrupted after 2 h, although many apparently intact particles that either excluded or included stain were also seen (Figure 6). In some experiments, 100–200 μg/ml proteinase K for 2 h at 4°C also led to an opening of the majority of the particles, as seen by an immunoblotting analysis of p39 and p4a (not shown). Collectively, these data argued that whereas the IMV has an inherently high resistance to proteases, at a certain threshold of activity the particle opens. The simplest interpretation of these data is that the outer cisterna of the IMV is sealed by a proteinaceous structure, although other interpretations cannot be ruled out. We stress that we have not yet seen any convincing evidence of any potential pore or other notable local structures on the IMV surface by cryo EM.

Extracellular enveloped virus (EEV)

The extracellular form of the IHD-J strain of vaccinia was purified from the medium of (the relatively high EEV yielding) rabbit RK13 cells and examined by cryo EM.

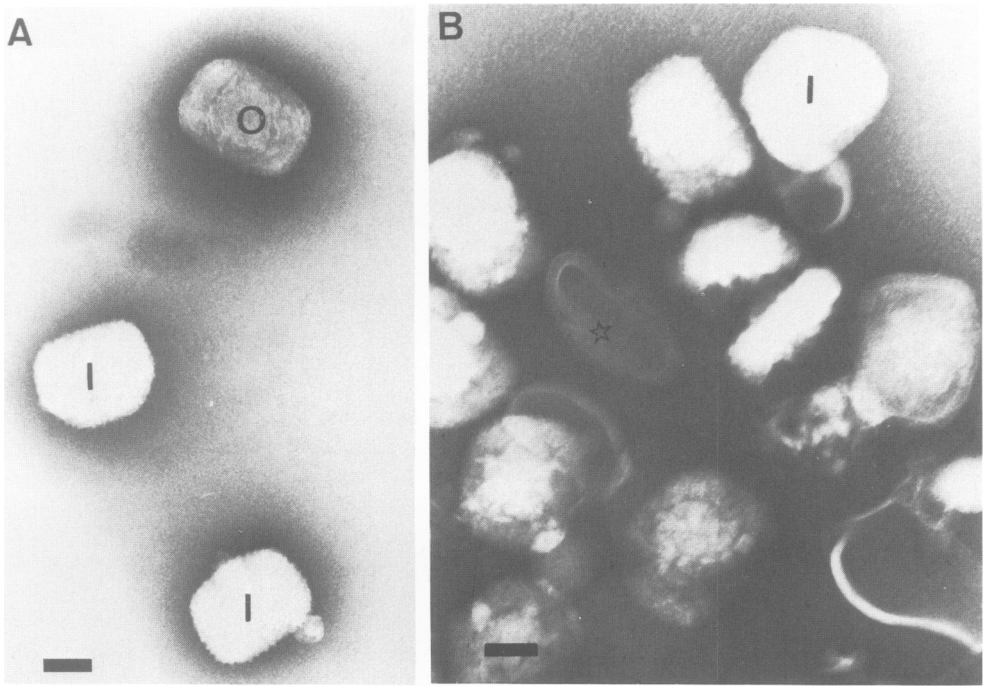

Fig. 6. Negative staining of vaccinia virus IMV. (**A**) A control virus preparation with two intact (I) particles that exclude stain and one open (O) but structurally intact particle that stain has entered. (**B**) A preparation treated in suspension with 200 μg/ml trypsin for 2 h showing one particle that we classify as normal and intact (I). The remainder either appear disrupted or include stain. The star indicates a side view of a particle into which stain has entered (bars = 100 nm).

In agreement with the current ideas on this viral form, these particles appeared to have one additional membrane bilayer that was clearly resolved (Figure 8A). However, in only few EEV particles did this membrane uniformly and tightly surround the particle and, even in this case, the interaction between the outer membrane and the underlying IMV was rather loose. In most cases, the membrane appeared to have little contact with the IMV and was often disrupted (Figure 8A; see also Payne and Kristenson, 1979). A brief fixation (seconds) of the EEV adsorbed to the grid with 0.5% glutaraldehyde increased the fraction of intact EEV particles considerably. When the outer membrane was removed completely, the surface of some of the underlying IMVs was much rougher in texture (Figure 8B) than the surface of purified IMV (Figure 2A). This surface appearance of the IMV resembled the structures described earlier as surface tubular elements by Stern and Dales (1978). The significance of these structures remains to be established.

Because of this tendency for the EEV to disrupt, we decided to investigate the topology of some key membrane proteins using the immunogold method in the absence of any treatment. In any one preparation, one could clearly identify both intact and disrupted particles. In these experiments, the structure of underlying IMV was rarely affected (except for the sometimes rougher surface texture, as mentioned).

Immunolabelling of EEV

For the EEV, we selected two antibodies which pilot experiments revealed to be especially interesting. The first was p42 (Table I) (Englestadt *et al.*, 1992; Isaacs *et al.*, 1992; Wolffe *et al.*, 1993). This protein is enriched in TGN-derived membranes that wrap around the IMV to form the IEV, the precursor of the EEV (see Figure 9). According to current ideas, the IEV fuses with the plasma membrane, thereby releasing the EEV (Payne, 1980; Schmelz *et al.*, 1994). As a result, lumenal epitopes that are buried within the wrapping cisterna become exposed on the surface of the EEV (see Figure 9).

The bulk of p42, like haemagglutinin (Shida, 1986; Schmelz *et al.*, 1994), should be exposed on the outside of the EEV, with the predicted small cytoplasmic domains of these proteins lying directly above the IMV. As expected from this model, a monoclonal antibody against p42 labelled the outside of the outer membrane of the EEV (Figure 8D). In those cases where the membrane was

Table II. Effect of proteases on IMV as seen by negative staining

	Percentage of total[a]		
	Intact	'Open'	Disrupted
Control	89	6	6
Proteinase K:			
100 μg, 1 h	88	9	3
200 μg, 1 h	85	10	5
100 μg, 2 h	89	1	10
200 μg, 2 h	83	2	15
Trypsin:			
100 μg, 1 h	92	4	4
200 μg, 1 h	75	6	19
100 μg, 2 h	71	25	4
200 μg, 2 h	8	27	65

[a]For each value, a total of 200 particles were counted. Examples of intact particles as well as particles that appear intact but 'open' to stain are shown in Figure 6A. Disrupted particles were defined as particles with gross morphological alterations (see Figure 6B).

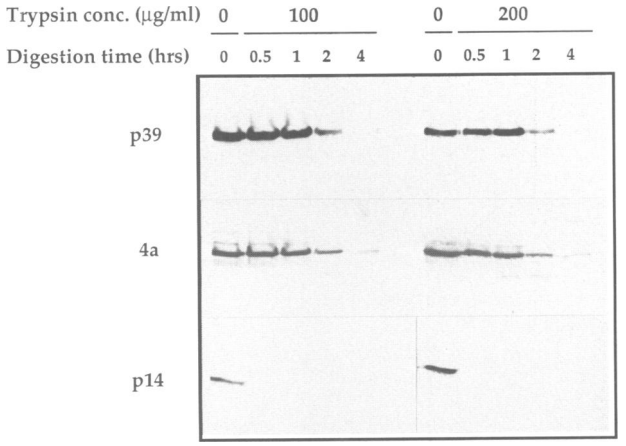

Fig. 7. Protease treatment of purified IMV. The virus was treated for different times with two concentrations of trypsin at 37°C. Immunoblots are shown for the core proteins, p39 and 4a and the IMV surface protein, p14. While the outer surface protein p14 is completely digested at the earliest time points, p39 and 4a resist significant degradation until 2 h. After 4 h, both proteins are essentially completely digested.

disrupted, the newly exposed surface was clearly devoid of labelling (not shown). However, this newly exposed surface, as expected, labelled strongly for the IMV surface protein p14 (Figure 8C). The second interesting protein we examined in the EEV was p37 (Table I) (Payne, 1978; Hiller and Weber, 1985; Hirt and Hiller, 1986) that is essential for IEV/EEV formation (Blasco and Moss, 1991). The available biochemical data argue that this protein, which has covalently bound palmitate, is an integral membrane protein, although it has not been established whether the protein is inserted into the rough ER or, as favoured by Hiller and Weber (1985) based on immunofluorescence microscopy analysis, whether it somehow inserts directly into Golgi membranes by a post-translational mechanism.

Labelling of thawed cryosections of vaccinia-infected cells shows that Golgi/TGN as well as the wrapping membranes and the EEV are enriched for p37 (Schmelz *et al.*, 1994). The data obtained, using a combination of immunogold labelling for p37 followed by cryo EM, argue that in the EEV this protein is localized to the space between the outer membrane and the surface of the IMV. Thus, the α-p37 had no access to its antigen in intact EEV (in contrast to the α-p42) but, following disruption/vesiculation and resealing of the outer membrane, there was strong labelling of the now exposed cytoplasmic side of the membrane (Figure 8E). These data are summarized schematically in Figure 9).

Discussion

Here we have studied the structure of vaccinia virus by cryo EM and, in particular, taken advantage of a recent finding by Cyrklaff *et al.* (1994) which shows that particles floating at the water–air interphase on a holey EM grid will remain there for the time needed to replace all the solutions simply by gentle changes of the underlying solvent. We adapted this technique for combining the advantages of immunogold labelling with the high resolution structural preservation that is obtainable routinely using cryo EM (Dubochet *et al.*, 1988).

Using this novel approach, we investigated both the structure and the topology of some key proteins in both the IMV and EEV forms of the poxvirus vaccinia, which probably represents the most complex form of all viruses. For the IMV, our work extends the preliminary findings of Dubochet *et al.* (1994) who first described the appearance of the IMV by cryo EM. The images in the study of Dubochet *et al.* supported the notion that the IMV has two membrane-like 'layers'. Further, they confirmed earlier data from negative staining EM that there are prominent, spike-like projections visible in IMV in images of conventional thin sections, as well as in vitrified preparations, which appear to be on the surface of virus treated with NP-40 plus DTT, the chemically prepared viral 'core'. The latter view is supported by our data in this study, which also show a correlation between the presence of the spikes on the core surface, that is exposed by DTT treatment, and a strong surface labelling for p39. Both the presence of spikes as morphological entities and labelling of their surface with α-p39 are also evident on the natural viral cores isolated during the infection process (Snijder *et al.*, in preparation). The strong labelling for p39 on the surface of the NP-40/DTT-prepared cores, on the core surface exposed after DTT alone and on the 'natural' cores argues that the same surface becomes exposed in all three conditions.

The model which emerges from the present study, in conjunction with our earlier data (Sodeik *et al.*, 1993), is shown in Figure 1A. This model argues that the tightly apposed cisterna, which incompletely surrounds the spherical IV, overlays the major spike-like projections that protrude from the surface of the viral core. This scheme is the simplest way to explain how DTT leads to the exposure of epitopes for p39, which is a cytosolic protein, on the surface of the core. We presume that DTT, a potent reducing agent, disrupts intra-lumenal disulphide bounds that stabilize the membrane–membrane interactions of the cisterna. According to current dogma, disulphide bonds can only form in the oxidizing environment of the ER and not in the highly reducing environment of the cytosol (Hwang *et al.* 1992; Doms *et al.* 1993). The images of the DTT-induced disruption process lead us to suggest that the IMV outer cisterna does not fuse with itself but is rather interrupted in some way.

The notion that the outer cisterna of the IMV is not fused together (as in Figure 1Ai) was also supported by the experiments with proteases showing that, whereas the IMV particles resisted relatively high concentration of protease for relatively long periods, above a certain threshold of protease activity viral core proteins became almost completely accessible to digestion. We tentatively propose, therefore, that the IMV outer cisterna is 'glued' together by a (relatively protease-resistant) proteinaceous structure. Since we have failed to see convincing evidence of any 'pore' structure (Figure 1Aii) by cryo EM, we speculate that the ends of the cisterna may be sealed by a protein 'plug' or 'focal contact' that tightly glues the end of the cisterna with the rest of the (same) cisterna (Figure 1Aiii).

The second important question raised by this study is the nature of the membrane-like electron-dense layer that

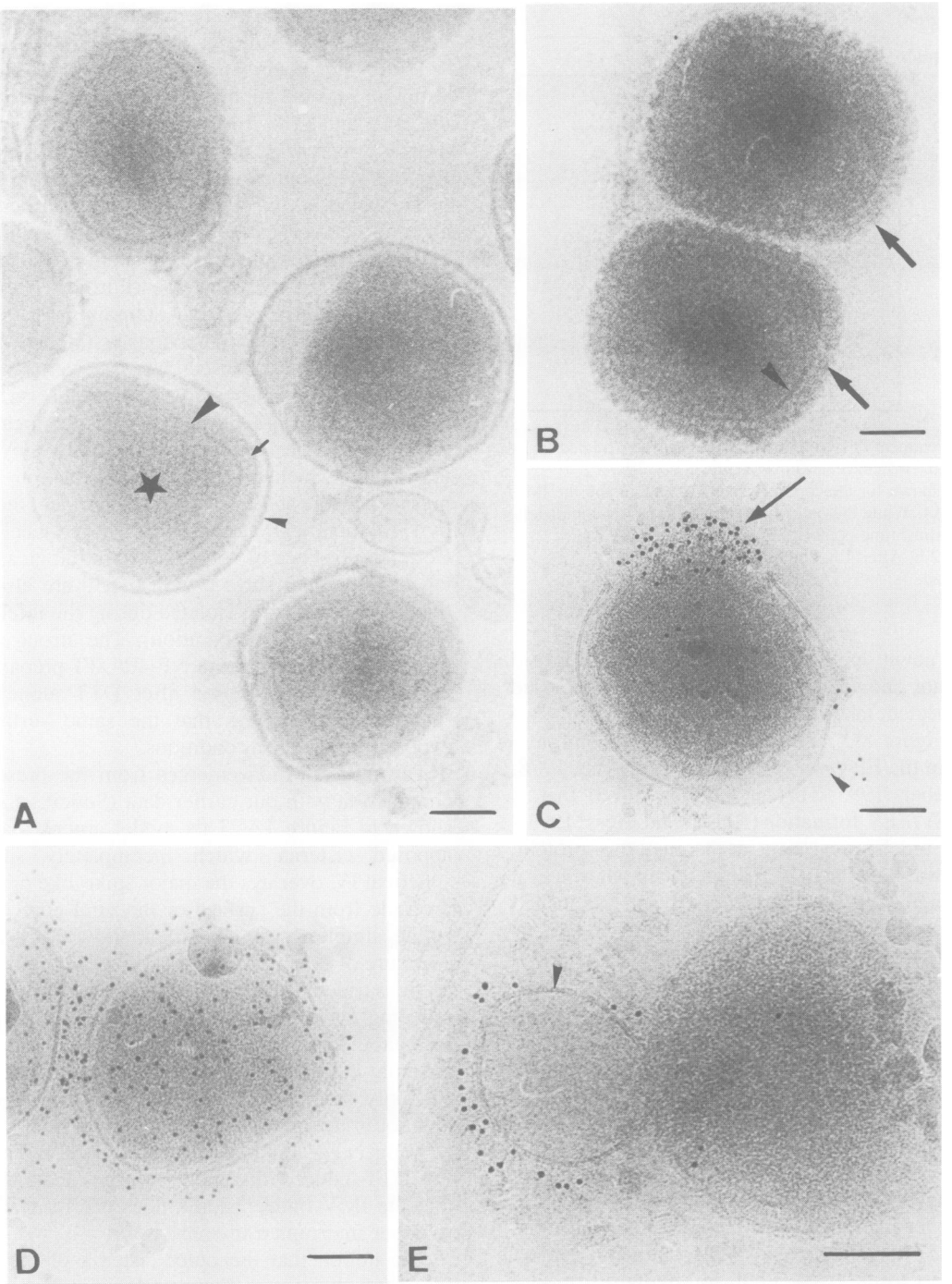

Fig. 8. Cryo EM of EEV. The EEV has one additional membrane relative to the IMV (Figure 2A). The outer membrane (small arrowheads) is extremely fragile in isolated preparations. (**A**) Untreated EEV; this preparation was taken directly from the extracellular medium of infected RK13 cells without centrifugation and vitrified. The asterisk depicts one of relatively few particles where the outer membrane remained intact. Very often they appear as shown in (**B**). In this example, the outer membrane has been removed exposing the outer surface of the IMV. We have no explanation for the ruffled appearance of these particles, which contrasts with the smooth appearance of isolated IMVs (see Figure 2A), but note the resemblance to the so-called surface tubular elements seen in classical negative stain preparations of IMV. In (**C**) the preparation was labelled with α-p14. Whereas this protein is not exposed in undisrupted particles, following disruption (in this case partial disruption) the epitopes for p14 are exposed and accessible for labelling. (**D**) Particles that have been immunolabelled with α-p42 showing the strong surface labelling on the outside of the EEV. (**E**) Whereas intact EEV does not label with α-p37, disrupted particles expose the cytoplasmic aspect of the outer membrane and become labelled (bar = 100 nm).

is clearly seen beneath the spike layer of the cores, both in vitrified specimens (Dubochet *et al.*, 1994; this study) and in thawed cryosections of IMV (Sodeik *et al.*, 1993). We intend to address this question, is it a membrane, by analysing the biochemical composition of cores produced during the infection process. As shown in this study, an obvious candidate protein that may at least comprise part of the core surface spikes is p39.

The ability of reducing agents to simulate an uncoating process may be of physiological significance. The available

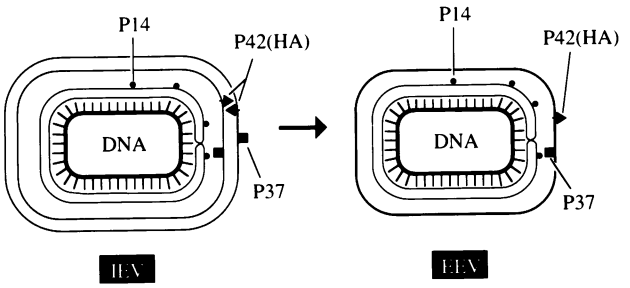

Fig. 9. Model to show the membrane topology in the IEV and EEV. The IMV acquires two additional membranes from the TGN to form the IEV. The outer membrane of the IEV is lost upon fusion with the cell membrane and the EEV is released into the extracellular medium. The bulk of p42 and HA are in the lumen of the IEV and become exposed on the surface of the EEV. In contrast, p37 is cytoplasmically disposed and is not exposed on the surface of the EEV unless the particles are disrupted. p14, which covers the surface of the underlying IMV, may interact with p37 although, until now, no evidence for such an interaction has existed.

data on the infection process for both IMV and EEV, while not definitive, have been interpreted as evidence for a fusion process in both cases (Armstrong *et al.*, 1973; Granados, 1973; Chang and Metz, 1976; Payne and Norrby, 1978; Doms *et al.*, 1990). If the EEV fuses with the plasma membrane, it would release an intact IMV into the cytoplasm. Our data now provide a plausible explanation for how such viruses could begin to disassemble as soon as they are exposed to the reducing environment of the cytosol. Such a view would also agree with the studies of Munyon *et al.* (1967), who showed that, while intact IMV cannot undergo the remarkable *in vitro* transcription process that is observed with pure cores, treatment of IMV with either DTT or 2-β-ME (in the absence of detergents) also leads to significant increases in the measured *in vitro* transcription rates.

The novel cryo EM approach also provided interesting data with respect to the EEV. Whenever we have isolated this form and examined it by either negative staining or following aldehyde fixation by cryosectioning, we were always surprised at the extreme lability of these particles. Unexpectedly, this lability was also evident in the cryo EM images, even when the virions were taken from the extracellular medium without centrifugation and in the absence of chemical fixation. That aldehyde fixation facilitated the preservation of these particles suggests that at least a part of the disruption we observed occurs during the storage and/or labelling steps. Only a minority of the particles had a complete and intact outer membrane and, even in those cases, this membrane did not appear to interact tightly with the surface of the IMV. The presence of this loose outer membrane on the physiologically most important infectious form of vaccinia (Payne, 1978) is surprising. In the simplest model, one might argue that this outer membrane is simply a transient coat that is lost in order to expose the IMV prior to infection. However, such a phenomenon would be difficult to reconcile with experiments showing that antibodies against IMV block infection of the IMV but fail to prevent infectivity of EEV particles (Payne, 1980). This view is also inconsistent with the fact that purified EEV enter cells more rapidly than does the IMV (Payne and Norrby, 1978; Doms *et al.*, 1990). Moreover, there are significant differences in the susceptibility of IMV and EEV to both temperature and metabolic inhibitors (Payne and Norrby, 1978).

A possible solution to the apparent paradox that the most infectious form of vaccinia is surprisingly labile, at least relative to the more robust IMV, comes from older (Stokes, 1976; Hiller *et al.*, 1979) and more recent (Cudmore *et al.*, 1995) observations on the mechanism by which the EEV exits from infected cells. These data argue that the IEV, the intracellular precursor of the EEV, is propelled through the cell by an actin-based tail structure (Cudmore *et al.*, 1995) similar to the structure first described for *Shigella* (Clerc and Sansonetti, 1987) and subsequently for *Listeria* (Tilney *et al.*, 1990; Theriot, 1994; for a review, see Cossart, 1995). The actin tail then somehow propels the IEV to the tip of a newly formed microvillus. One can speculate that the IEV subsequently fuses with the plasma membrane at the tip of the microvillus, releasing the EEV to the outside. Thin section EM images suggest that the EEV remains attached to the plasma membrane for extended periods, since they are relatively easy to find in thin sections. The EEV can then fuse with and infect a neighbouring, uninfected cell. In this scenario, an important extracellular role of the EEV would be as a transient and perhaps predominantly cell-associated form that facilitates rapid cell to cell transfer. In further agreement with this view is the recent identification of a distinct class of plasma membrane-attached EEV, the CEV (cell-associated virus) form (Blasco and Moss, 1992).

Our immunolabelling data on the EEV fit clearly into existing models. Thus, the EEV has one extra membrane relative to the IMV and that membrane is enriched in p42 (Englestadt and Smith, 1993; Schmelz *et al.*, 1994), p21 (Duncan and Smith, 1992; Payne, 1992), haemagglutinin (Shida, 1986) and a recently identified 43–50 kDa membrane protein (Parkinson and Smith, 1994). All these proteins are exposed predominantly on the outer surface of the EEV and, for p42, we show this directly in this study. More significantly, we showed that p37 (Hiller *et al.*, 1981; Hiller and Weber, 1985; Schmutz *et al.*, 1991; Schmelz *et al.*, 1994) is exposed to its antibody on the inner aspect of the outer membrane of the EEV only following disruption, in agreement with the recent biochemical data of Schmutz *et al.* (1995). This protein has been postulated to interact with a protein(s) on the surface of the IMV. The best candidate for the latter is, as previously proposed by Rodriguez and Smith (1990), p14, which here became exposed to its antibody only following disruption of the outer membrane of the EEV, as expected if the outer membrane directly covers the surface of the IMV.

We believe that the novel approach of immunogold labelling, in combination with cryo EM of vitrified particles, will be a useful approach for any particle in the range of 50–500 nm. Since the antibody–gold complex is relatively large (minimum size ~20 nm) we emphasize that this is not a high resolution labelling technique *per se*. Available methods that could be applied to improve the spatial resolution of the immunolabelling would give only modest, but nevertheless important, gains (Griffiths, 1993). However, by combining the immunolabelling with methods to disrupt or digest biological particles in a controlled fashion, we believe this approach can best be

used for identifying layers or domains in other complex macromolecular structures such as nuclear pores, centrioles, kinetochores, or perhaps defined fragments of chromosomes, under conditions which avoid most of the artefacts associated with more conventional EM methods.

Materials and methods

Antibodies and protein A–gold

The following antibodies were used: mouse monoclonal α-p14 (Dallo *et al.*, 1987; Sodeik *et al.*, 1995) and rabbit α-p39 provided by Dr M.Esteban; mouse monoclonal α-p42 (Schmelz *et al.*, 1994) and mouse monoclonal α-p37 (Schmelz *et al.*, 1994) provided by Dr G.Hiller. Protein A–gold was purchased from Dr Jan Slot (University of Utrecht, Stichting MEMO, Utrecht, The Netherlands).

Cells and viral strains

Preparation of IMV. HeLa cells (ATCC CCL2) were grown in Eagle's minimal essential medium (MEM) supplemented with 10% fetal calf serum (FCS; heat-inactivated), non-essential amino acids, 2 mM glutamine, 100 U/ml penicillin and 100 μg/ml streptomycin. The cells were grown as adherent cultures at 37°C in a 5% CO_2 incubator for 2 days to 80% confluency. For the preparation of purified IMV, we used both wild-type WR virus and a WR deletion mutant (vRB12), lacking the EEV protein p37 (gene F13L; Blasco and Moss, 1992) that fails to produce IEV and EEV. Since this deletion mutant does not spread readily from cell to cell, special care was taken to infect cells at a relatively high multiplicity of infection (m.o.i.). The use of this vRB12 mutant ensures that IMV preparations are devoid of EEV particles.

The routine procedure was to infect four flasks (175 ml) at an m.o.i. of ~3 for 48 h, after which the IMV was released by freeze–thawing. This virus preparation was used to infect six plates (24×24 cm) of 70% confluent HeLa cells. This generally led to complete cytopathic effects at 48 h post-infection. The cells were harvested by scraping and centrifuged for 10 min at 1500 r.p.m. The cells were broken with 12 strokes of a dounce homogenizer and the nuclei removed by centrifugation at 1000 *g*. The IMV subsequently was purified by pelleting at 24 000 r.p.m. through a 36% sucrose cushion (in 10 mM Tris pH 9.0), followed by sedimentation at 15 000 r.p.m. for 17 min in a 25–40% sucrose gradient using an SW27 rotor, and the subsequent band finally concentrated by pelleting for 30 min at 24 000 r.p.m. in a SW40 Beckman rotor. (Doms *et al.*, 1990). Such IMV preparations usually contained from 10^{10} to 10^{11} particles/ml. All cell culture material was obtained from Gibco, GIBCO BRL (Gaithersburg, MD).

Preparation of EEV. Most of the virus present in the medium from infected cells 24 h post-infection is EEV (Payne and Kristenson, 1979). Since EEV is a very fragile form of vaccinia and has the tendency to lose its outer membrane when exposed to mechanical stress, we tried to avoid any unnecessary manipulation. For many, but not all, experiments we took the EEV directly from the medium of IHD-J-infected RK13 cells 48 h after infection without further purification (Payne, 1979). In order to increase the number of viral particles, we reduced the amount of medium to a minimum. Confluent monolayers in 25 cm^2 flasks were infected with IHD-J and incubated in 2 ml of MEM containing 2.5% FCS. Sometimes the medium was clarified by low speed centrifugation and the amount of free virions in the medium estimated by negative staining.

Partial disruption of virus particles. For this, the particle suspension was applied to a perforated carbon grid and allowed to adsorb for 3–10 min, depending on particle concentration. The grid was then washed briefly in 10 mM Tris pH 9.0 and incubated on 20 mM DTT in 10 mM Tris pH 9 at 37°C or room temperature for 5–30 min in a humid chamber. The grids were rinsed subsequently with 10 mM Tris buffer (pH 9) and either frozen immediately or used for further labelling experiments as described below.

Protease digestion studies

Sucrose gradient-purified IMV was mixed with an equal volume of 200 or 400 μg/ml trypsin, in 10 mM Tris, pH 9, containing 20 mM $CaCl_2$. Alternatively, 200 or 400 μg/ml protease K on ice was used. The final concentrations of proteases used were 100 or 200 μg/ml. Incubation at 37°C was continued for 30, 60, 120 or 240 min. Subsequently, digestion was blocked for 10 min on ice using 1 μl of aprotinin stock solution (4 mg/ml) and 1 μl of bovine trypsin inhibitor (20 mg/ml) (Sigma) in the case of trypsin or 2 mM phenylmethylsulphonyl fluoride (Sigma) for the protease K. The samples were snap-frozen in liquid nitrogen and stored at –20°C before analysis using 15% SDS–PAGE. Samples were thawed rapidly by incubation at 95°C with Laemmli sample buffer, the gels run and the proteins transferred to nitrocellulose and blotted for p39, p14 and 4a (a gift from Dr D.Hruby; see vanSlyke *et al.*, 1991), as described (Ericsson *et al.*, 1995)

For negative staining, aliquots of the virus plus protease were adsorbed to glow-discharged, carbon-coated grids, rinsed briefly with distilled water and negatively stained with 2% uranyl acetate.

Labelling of virus particles

Labelling experiments were performed as follows: after the 3–5 μl drop of particle suspension had been left for a given time on the grid (the side coated with the perforated carbon film), the grid was washed on 1 ml droplets of HEPES buffer (100 mM pH 7.4) four times for 2 s and once for 2 min. The grid subsequently was placed on a small droplet (5–10 ml) of antibody solution for 15–30 min, followed by a further washing step with buffer (4× 2 s and 1× 2 min). The grid was then subjected to a protein A–gold solution for 15 min and washed (4× 2 s and then 2× 2 min). In the case where antibodies which do not bind to protein A (i.e. mouse primary antibodies) were used, the grid was incubated on a secondary antibody solution, prior to another washing step, before it was exposed to the protein A–gold solution. For double labelling, we followed the general regime used for labelling of cryosections with somewhat reduced incubation times. Blotting and vitrification took place as described below (Slot *et al.*, 1991). In the few cases where we tested the use of fixatives, the grids were either placed briefly (seconds to minutes) on drops of formaldehyde solution (4% in 100 mM HEPES, pH 7.4) or glutaraldehyde solution (0.5% in 100 mM HEPES, pH 7.4).

Specimen preparation for cryoelectron microscopy

The thin film vitrification method is described in detail elsewhere (Dubochet *et al.*, 1988; Roos and Morgan, 1990). A 3–5 μl droplet of suspension was put on a grid supporting a perforated carbon film with hole diameters between 2 and 5 mm. The drop was left on the grid for 1–3 min in the case of IMV and up to 10 min in the case of EEV. Blotting paper (Whatmann no. 1) was then firmly applied to one side of the grid for ~1 s. The plunger holding the grid was immediately released and, within ~0.1 s, the grid was plunged into a liquid ethane slush cooled with liquid nitrogen, thus vitrifying the thin liquid film.

Cryoelectron microscopy

The vitrified samples were either stored in liquid nitrogen or observed immediately. Transfer and observations were made with side-entry, cryo-transfer holders [Gatan 626 (Gatan, Varrendale, PA) and Oxford Instruments, CT-3500 (Oxford Instruments, Oxford, UK)] in a specially adapted cryoelectron microscope, the Jeol-2000EX (JEOL, Tokyo, Japan, equipped with a Gatan TV camera, model 622-0600 with an image intensifier). The microscope has an efficient blade-type anti-contaminator. Observations were made under minimum irradiation conditions at magnifications ranging from ×3000 to 40 000 and at 3.5–10.5 mm under focus. Micrographs were recorded on Kodak SO-163 electron microscopy film and developed in full-strength D-19 developer for 12 min (speed ~2.2 μm^2/electron×OD unit). Magnification was calibrated with a cross-grating replica, with an estimated error of 2%.

Acknowledgements

We would like to thank the following for their generous gift of antibodies: Dr M.Esteban for providing α-p14 and α-p39, Dr E.Niles for α-p32, Dr G.Hiller for α-p42 and α-p37 and Dr D.Hruby for α-4a. We are also grateful to Dr K.Simons for his critical comments on the manuscript.

References

Appleyard,G., Hapel,A.J. and Boulter,E.A. (1971) *J. Gen. Virol.*, **13**, 9–17.

Armstrong,J.A., Metz,D.H. and Young,M.R. (1973) *J. Gen. Virol.*, **21**, 533–537.

Blasco,R. and Moss,B. (1991) *J. Virol.*, **65**, 5910–5920.

Blasco,R. and Moss,B. (1992) *J. Virol.*, **66**, 4170–4179.

Chang,A. and Metz,D.H. (1976) *J. Gen. Virol.*, **32**, 275–282.

Clerc,P. and Sansonetti,P.J. (1987) *Immunology*, **55**, 2681–2688.

Cossart,P. (1995) *Curr. Opin. Cell Biol.*, **7**, 94–101.

Cudmore,S., Cossart,P., Griffiths,G. and Way,M. (1995) *Nature*, **378**, 636–638.
Cyrklaff,M., Adrian,M. and Dubochet,J. (1990) *J. Electron Microsc. Techniques*, **16**, 351–355.
Dales,S. (1963) *J. Cell Biol.*, **18**, 51–72.
Dales,S. and Mosbach,E.H. (1968) *Virology*, **35**, 564–583.
Dales,S. and Pogo,B.G.T. (1981) *Virology Monographs*. Springer-Verlag, Vienna.
Dales,S. and Siminovitch,L. (1961) *J. Biophys. Biochem. Cytol.*, **10**, 475–503.
Dallo,S., Rodriguez,J.F. and Esteban,M. (1987) *Virology*, **159**, 423–432.
Doms,R.W., Blumenthal,R. and Moss,B. (1990) *J. Virol.*, **64**, 4884–4892.
Doms,R.W., Lamb,R.A., Rose,J.K. and Helenius,A. (1993) *Virology*, **193**, 545–562.
Dubochet,J., Adrian,M., Chang,J.-J., Homo,J.-C., Lepault,J., McDowall,A.W. and Schultz,P. (1988) *Q. Rev. Biophys.*, **21**, 129–228.
Dubochet,J., Adrian,M., Richter,K., Garces,J. and Wittek,R. (1994) *J. Virol.*, **68**, 1935–1941.
Duncan,S.A. and Smith,G.L. (1992) *J. Virol.*, **66**, 1610–1621.
Easterbrook,K.B. (1966) *J. Ultrastruct. Res.*, **14**, 484–496.
Englestad,M. and Smith,G.L. (1993) *Virology*, **194**, 627–637.
Englestad,M., Howard,S.T. and Smith,G.L. (1992) *Virology*, **188**, 801–810.
Ericsson,M., Cudmore,S., Shuman,S., Condit,R.C., Griffiths,G. and Krijnse Locker,J. (1995) *J. Virol.*, **69**, 7072–7086
Granados,R.R. (1973) *Virology*, **52**, 305–309.
Griffiths,G. (1993) *Fine Structure Immunocytochemistry*. Springer Verlag, Berlin.
Griffiths,G. and Rottier,P. (1992) *Semin. Cell Biol.*, **3**, 367–381.
Hiller,G. and Weber,K. (1985) *J. Virol.*, **55**, 651–659.
Hiller,G., Weber,K., Schneider,L., Parajsz,C. and Jungwirth,C. (1979) *Virology*, **98**, 142–153.
Hiller,G., Eibl,H. and Weber,K. (1981) *J. Virol.*, **39**, 903–913.
Hirt,P. and Hiller,P. (1986) *J. Virol.*, **58**, 757–767.
Holowczak,J.A. and Joklik,W.K. (1967) *Virology*, **33**, 717–725.
Hwang,C., Sinskey,A.J. and Lodish,H.F. (1992) *Science*, **257**, 1496–1502.
Isaacs,S.N., Wolffe,E.J., Payne,L.G. and Moss,B. (1992) *J. Virol.*, **66**, 7217–7224.
Johnson,R.P.C. and Gregory,D.W. (1993) *J. Microsc.*, **171**, 125–136.
Joklik,W.K. (1964) *J. Mol. Biol.*, **8**, 262–276.
Kates,J.R. and McAuslan,B. (1967) *Proc. Natl Acad. Sci. USA*, **57**, 314–320.
Krijnse Locker,J., Ericsson,M., Rottier,P.J.M. and Griffiths,G. (1994) *J. Cell Biol.*, **124**, 55–70.
Munyon,W., Paoletti,E. and Grace,J.T.,Jr (1967) *Proc. Natl Acad. Sci. USA*, **58**, 2280–2287.
Parkinson,J.E. and Smith,G.L. (1994) *Virology*, **204**, 376–390.
Payne,L.G. (1978) *J. Virol.*, **27**, 28–37.
Payne,L.G. (1979) *J. Virol.*, **31**, 147–155.
Payne,L.G. (1980) *J. Gen. Virol.*, **50**, 89–100.
Payne,L.G. (1992) *Virology*, **187**, 251–260.
Payne,L.G. and Kristenson,K. (1979) *J. Virol.*, **32**, 614–622.
Payne,L.G. and Norrby,E. (1978) *J. Virol.*, **27**, 19–27.
Rodriguez,J.F. and Esteban,M. (1987) *J. Virol.*, **61**, 3550–3554.
Rodriguez,J.F. and Smith,G.L. (1990) *Nucleic Acid Res.*, **18**, 5347–5351.
Rodriguez,J.F., Paez,E. and Esteban,M. (1987) *J. Virol.*, **61**, 395–404.
Roos,N. and Morgan,A.J. (1990) *Cryopreservation of Thin Biological Specimens for Electron Microscopy: Methods and Applications*. Oxford Science Publications.
Shida,H. (1986) *Virology*, **150**, 451–462.
Schmelz,M., Sodeik,B., Ericsson,M., Wolffe,E.J., Shida,H., Hiller,G. and Griffiths,G. (1994) *J. Virol.*, **68**, 130–147.
Schmutz,C., Payne,G., Gubser,J. and Wittek,R. (1991) *J. Virol.*, **65**, 3435–3442.
Schmutz,C., Rindisbacher,L., Galmiche,M.C. and Wittek,R. (1995) *Virology*, **213**, 19–27.
Slot,J.W., Geuze,H.J., Gigengack,S., Leinhard,G.E. and James,D.E. (1991) *J. Cell Biol.*, **113**, 123–135.
Sodeik,B., Doms,R.W., Ericsson,M., Hiller,G., Machamer,C.E., von't Hof,W., von Meer,G., Moss,B. and Griffiths,G. (1993) *J. Cell Biol.*, **121**, 521–541.
Sodeik,B., Cudmore,S., Ericsson,M., Esteban,M., Niles,E. and Griffiths,G. (1995) *J. Virol.*, **69**, 3560–3574.
Stern,W. and Dales,S. (1976) *Virology*, **75**, 232–241.
Stewart,P.L., Burnett,R.M., Cyrklaff,M. and Fuller,S.D. (1991) *Cell*, **67**, 145–154.
Stokes,G.V. (1976) *J. Virol.*, **18**, 636–643.
Theriot,J.A. (1994) *Semin. Cell Biol.*, **5**, 193–199.
Tilney,L.G., Connelly,P.S. and Portnoy,D.A. (1990) *J. Cell Biol.*, **111**, 2979–2988.
vanSlyke,J.K., Whitehead,S.S., Wilson,E.M. and Hruby,D.E. (1991) *Virology*, **183**, 467–478.
Wolffe,E.J., Isaacs,S.N. and Moss,B. (1993) *Virology*, **67**, 4732–4741.

Received on November 24, 1995; revised on January 24, 1996